SUPPLEMENTARY DATA

Anti-Alzheimer potential of *Tamarindus indica*: An *in vivo* investigation supported by *in vitro* and *in silico* approach

Abeer H. Elmaidomy[1#], Usama Ramadan Abdelmohsen[2,3*#], Faisal Alsenani[4], Hanan F. Aly[5], Shams Gamal Eldin Shams[5], Eman A. Younis[5], Kawkab A. Ahmed[6], Ahmed M. Sayed[7], Asmaa I. Owis[1], Naglaa Afifi[1], Dalia El Amir[1]

[1]Department of Pharmacognosy, Faculty of Pharmacy, Beni-Suef University, Beni-Suef 62514, Egypt

[2]Department of Pharmacognosy, Faculty of Pharmacy, Minia University, Minia 61519, Egypt

[3]Department of Pharmacognosy, Faculty of Pharmacy, Deraya University, 7 Universities Zone, New Minia 61111, Egypt

[4]Department of Pharmacognosy, Faculty of Pharmacy, Umm Al-Qura University, Makkah 21955, Saudi Arabia

[5]Therapeutic Chemistry Department, National Research Centre (NRC), El-Bouth St., P.O. 12622 Cairo, Egypt

[6]Department of Pathology, Faculty of Veterinary Medicine, Cairo University, Giza, 12211, Egypt

[7]Department of Pharmacognosy, Faculty of Pharmacy, Nahda University, 62513, Beni-Suef, Egypt

*Corresponding author: Department of Pharmacognosy, Faculty of Pharmacy, Minia University, Minia 61519, Egypt, usama.ramadan@mu.edu.eg

# Those authors are equally contributed

Abstract

Tamarindus indica Linn., (Tamarind, F. Fabaceae) is one of the most widely consumed fruits in the world. The crude extract and different fractions of *T. indica* (*n*-hexane, dichloromethane, ethyl acetate, and *n*-butanol) were evaluated *in vitro* against DPPH scavenging, and AchE inhibition activities. Results showed that dichloromethane, and ethyl acetate fractions showed the highest antioxidant activities, with 84.78, and 86.96% DPPH scavenging using 0.10 ug/mL. While the *n*-hexane, dichloromethane, and ethyl acetate fractions, inhibited AchE activity in a dose dependent manner, where *n*-hexane fraction showed the highest inhibition at 20 µg/mL. The results were confirmed by subjecting *n*-hexane, dichloromethane, and ethyl acetate fractions *in vivo* in regression of the neurodegenerative features of Alzheimer's dementia in Aluminum-intoxicated rat model. Phytochemical investigation for those three fractions afforded two new diphenyl ether derivatives compounds **1-2**, along with five known ones. The structures of the isolated compounds had been confirmed using 1D, 2D NMR and HRESIMS analyses. The isolated compounds were subjected to extensive *in silico*-based investigation to putatively highlight the most probable compounds responsible for the anti-Alzheimer activity of *T. indica*. Inverse docking that was followed by molecular dynamics simulation (MDS) and binding free energy (ΔG) estimation suggested both compounds **1** and **2** to be promising AchE inhibitors. The results presented in this study may provide potential dietary supplements for the management of Alzheimer disease.

Keywords: Alzheimer; AchE; *in vitro;* docking*; in silico*; *Tamarindus indica.*

List of Contents

Figure S1. ^{1}H NMR spectrum of compound **1** measured in DMSO-d_6 at 400 MHz

Figure S2. DEPT-Q NMR spectrum of compound **1** measured in DMSO-d_6 at 100 MHz

Figure S3. ^{1}H NMR spectrum of compound **2** measured in DMSO-d_6 at 400 MHz

Figure S4. DEPT-Q NMR spectrum of compound **2** measured in DMSO-d_6 at 100 MHz

Figure S5. ^{1}H NMR spectrum of compound **3** measured in CD_3OD-d_4 at 400 MHz

Figure S6. DEPT-Q NMR spectrum of compound **3** measured in CD_3OD-d_4 at 100 MHz.

Figure S7. ^{1}H NMR spectrum of compound **4** measured in CD_3OD-d_4 at 400 MHz

Figure S8. DEPT-Q NMR spectrum of compound **4** measured in CD_3OD-d_4 at 100 MHz

Figure S9. ^{1}H NMR spectrum of compound **5** measured in CD_3OD-d_4 at 400 MHz

Figure S10. DEPT-Q NMR spectrum of compound **5** measured in CD_3OD-d_4 at 100 MHz

Figure S11. ^{1}H NMR spectrum of compound **6** measured in DMSO-d_6 at 400 MHz

Figure S12. DEPT-Q NMR spectrum of compound **6** measured in DMSO-d_6 at 100 MHz

Figure S13. ^{1}H NMR spectrum of compound **7** measured in $CDCL_3$-d at 400 MHz

Figure S14. DEPT-Q NMR spectrum of compound **7** measured in $CDCL_3$-d at 100 MHz

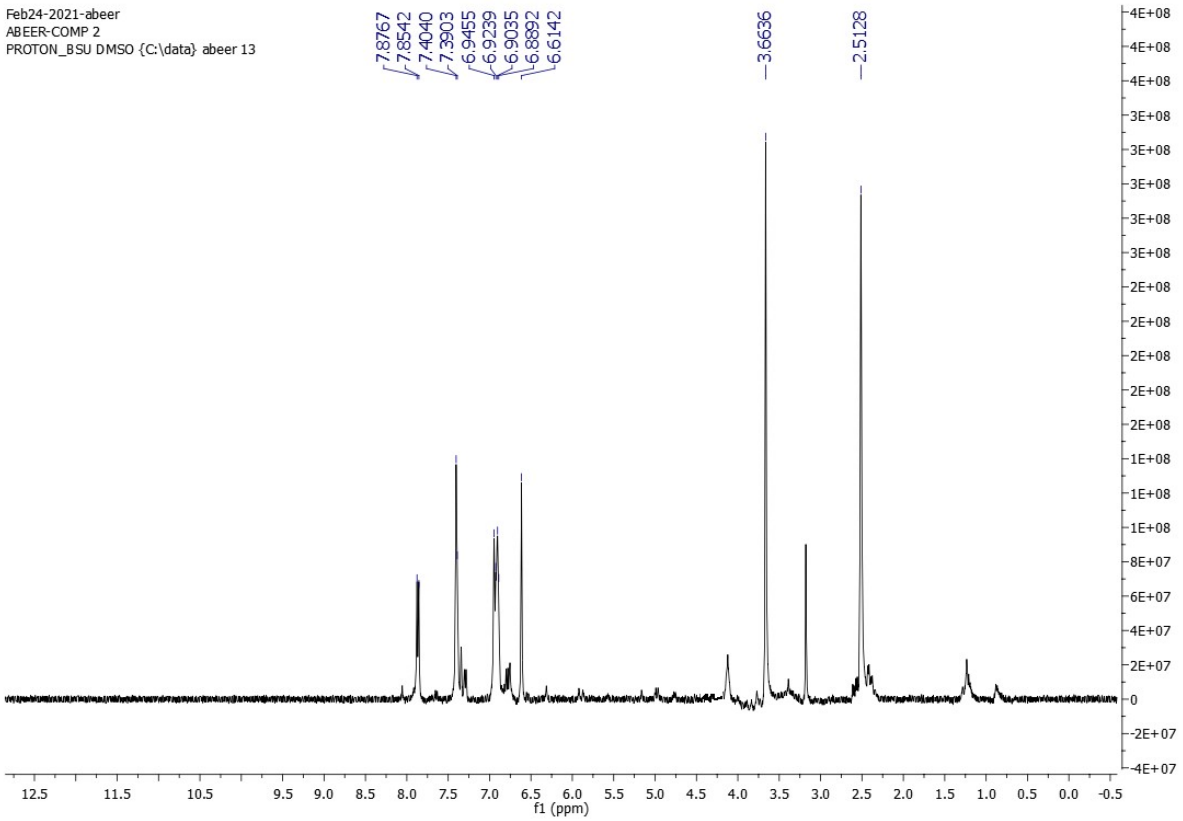

Figure S1. ^{1}H NMR spectrum of compound **1** measured in DMSO-d_6 at 400 MHz

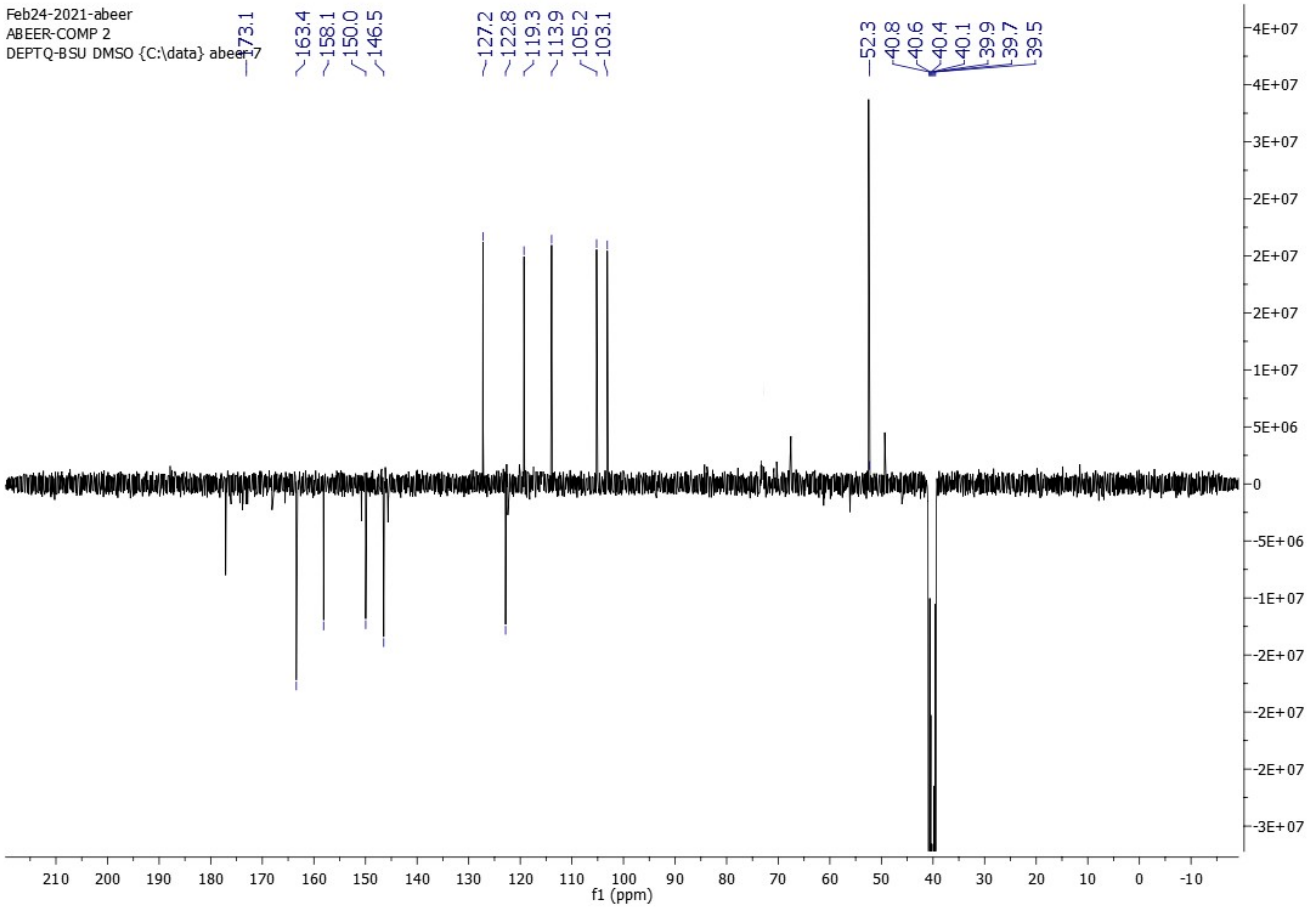

Figure S2. DEPT-Q NMR spectrum of compound **1** measured in DMSO-d_6 at 100 MHz

Figure S3. ^{1}H NMR spectrum of compound **2** measured in DMSO-d_6 at 400 MHz

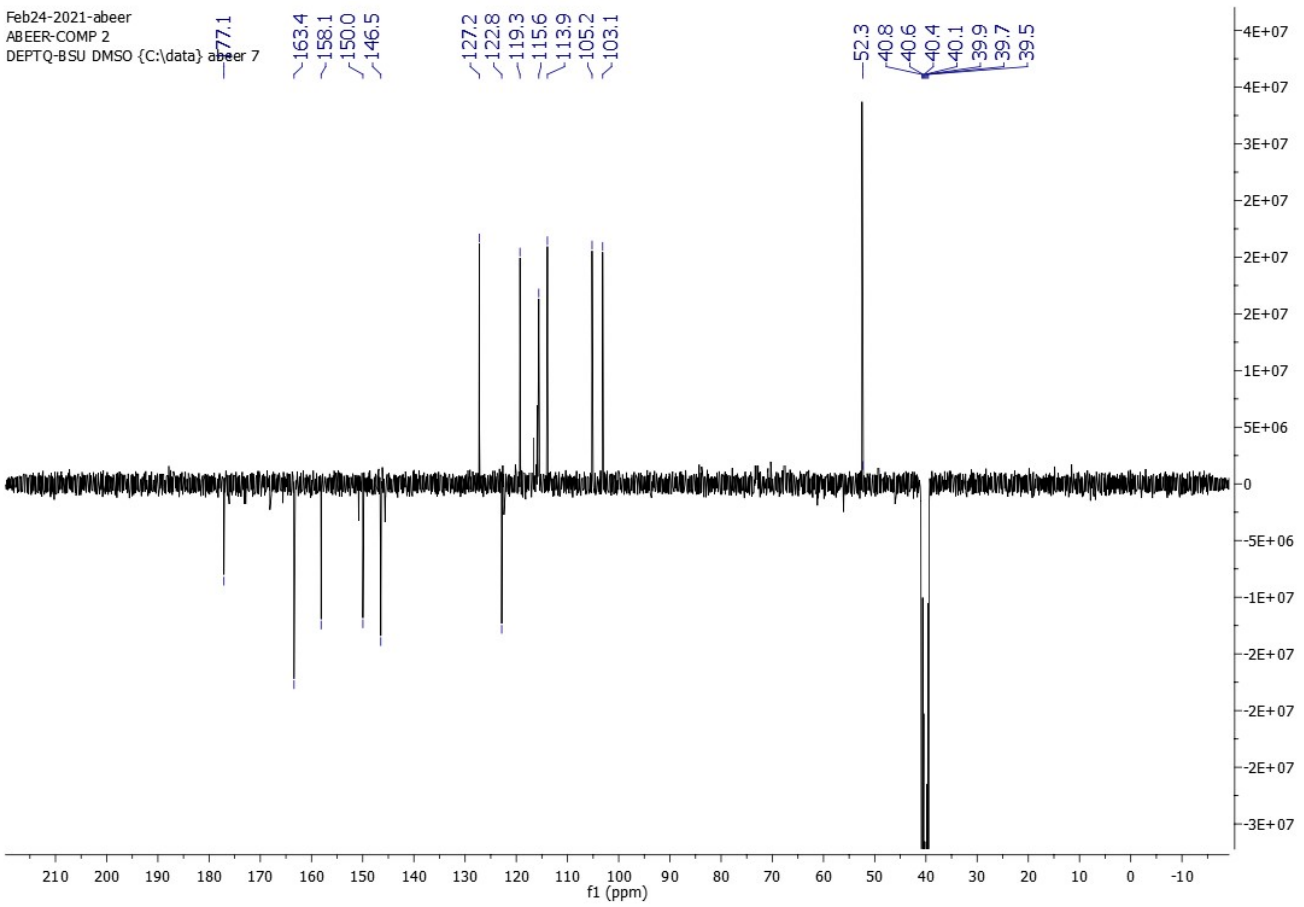

Figure S4. DEPT-Q NMR spectrum of compound **2** measured in DMSO-d_6 at 100 MHz

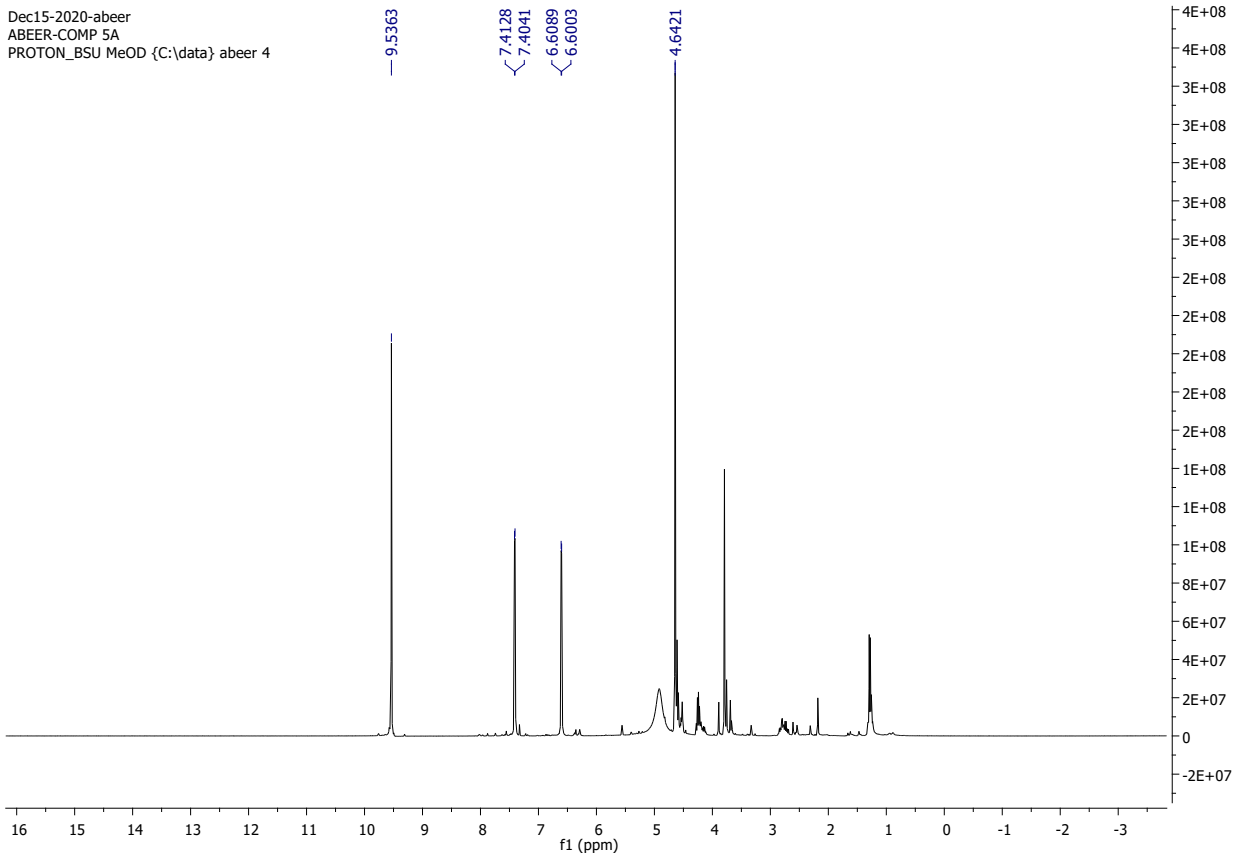

Figure S5. ^{1}H NMR spectrum of compound **3** measured in CD_3OD-d_4 at 400 MHz

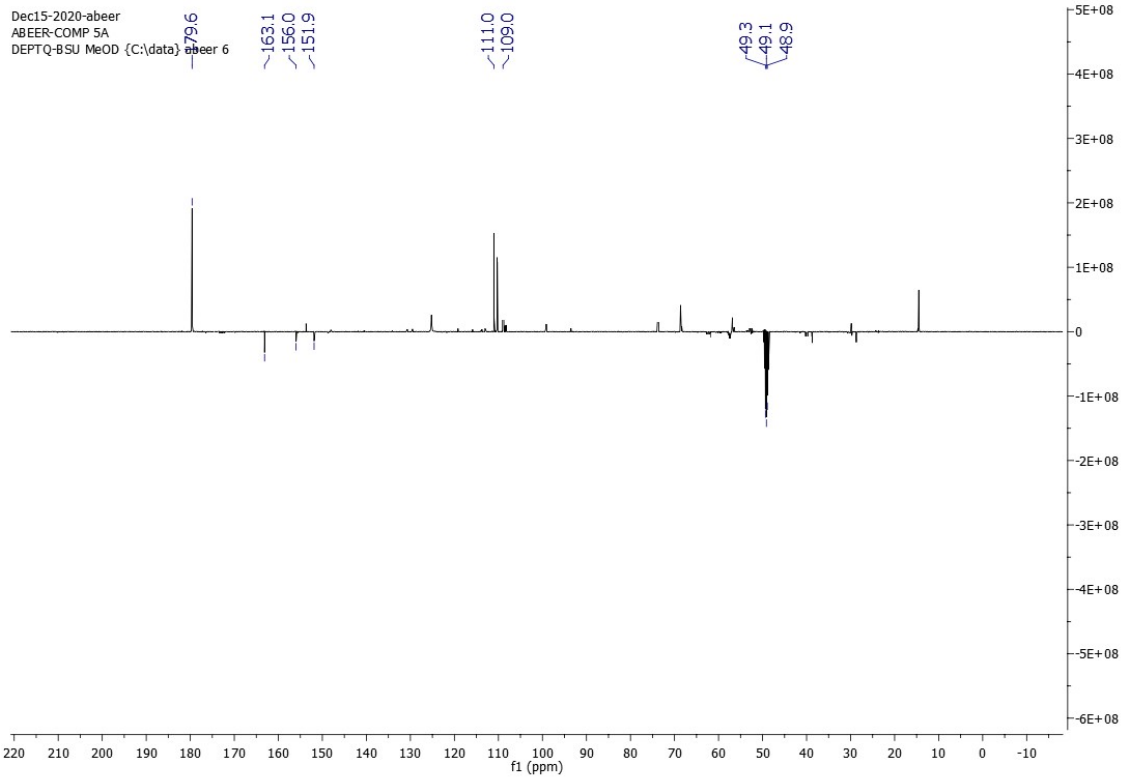

Figure S6. DEPT-Q NMR spectrum of compound **3** measured in CD_3OD-d_4 at 100 MHz.

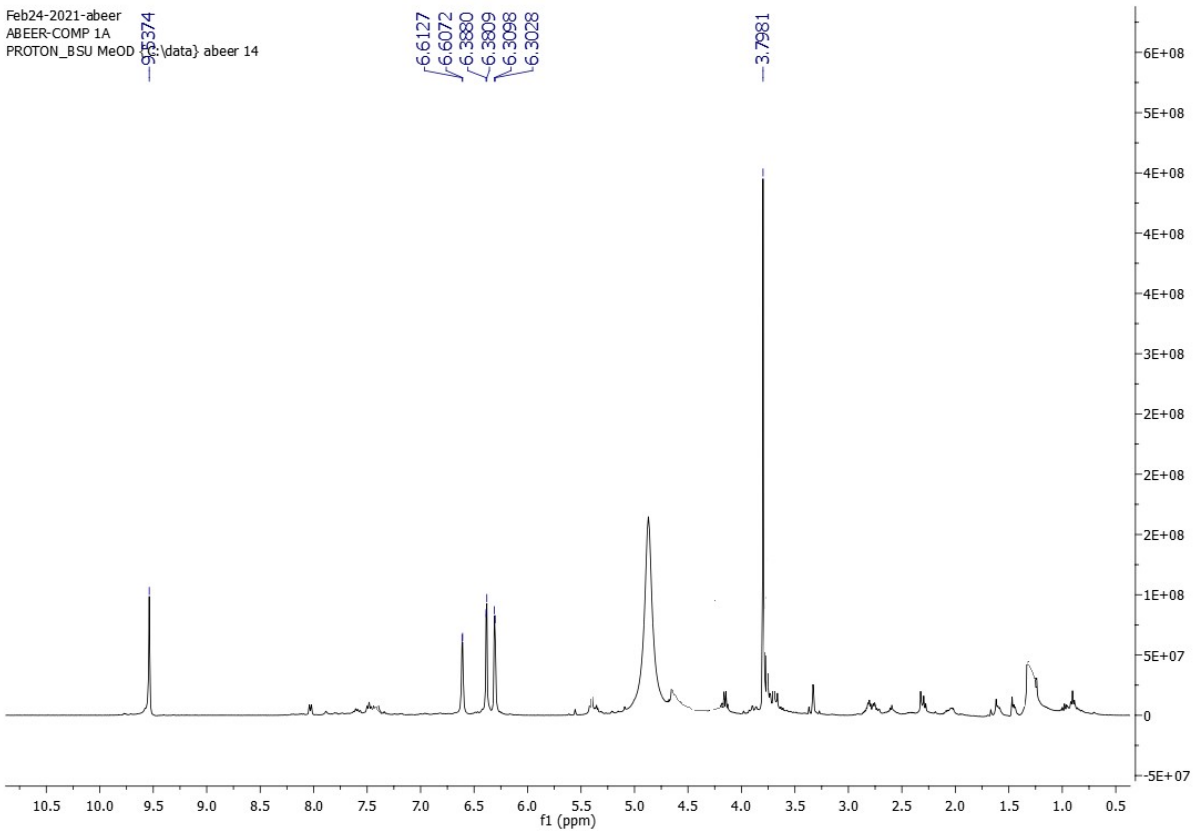

Figure S7. ^{1}H NMR spectrum of compound **4** measured in CD_3OD-d_4 at 400 MHz

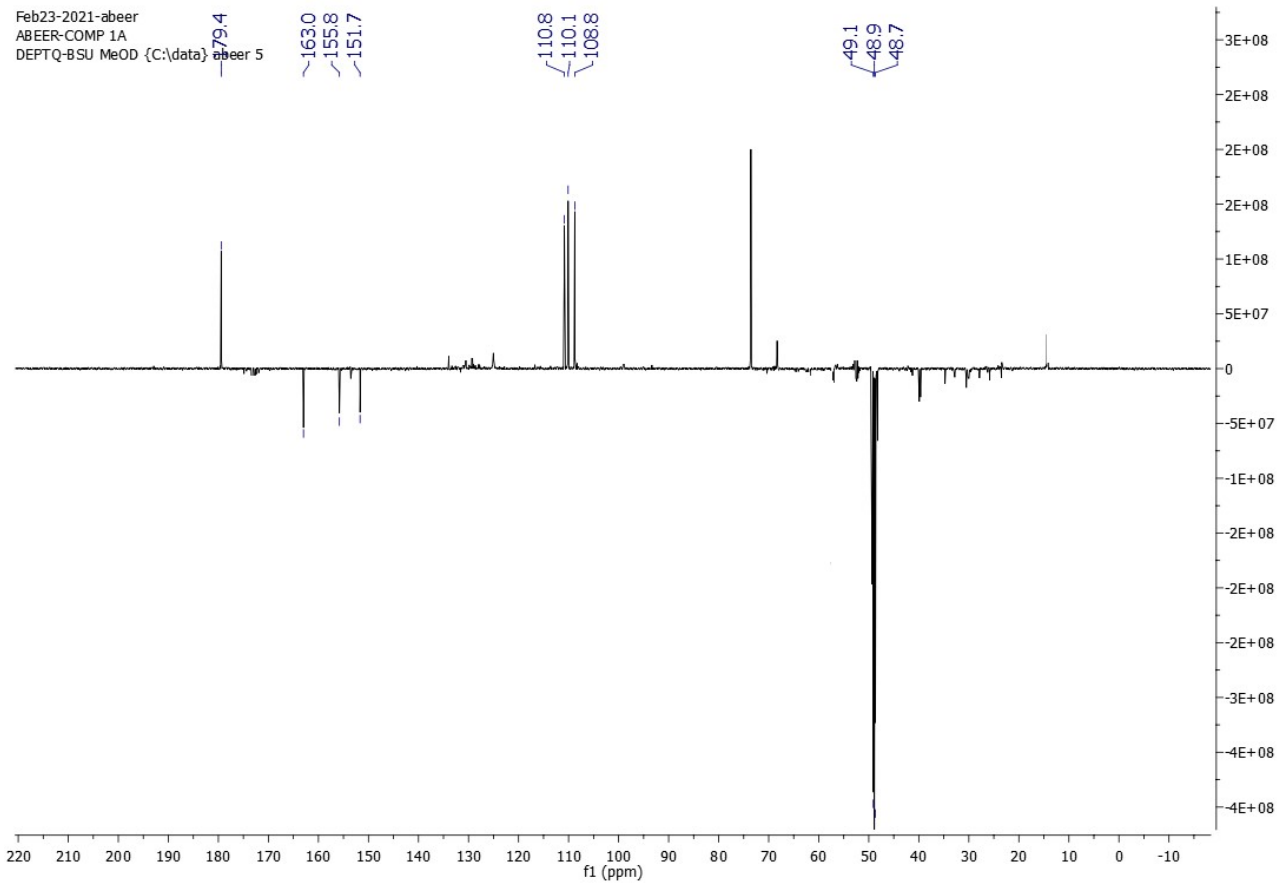

Figure S8. DEPT-Q NMR spectrum of compound **4** measured in CD_3OD-d_4 at 100 MHz

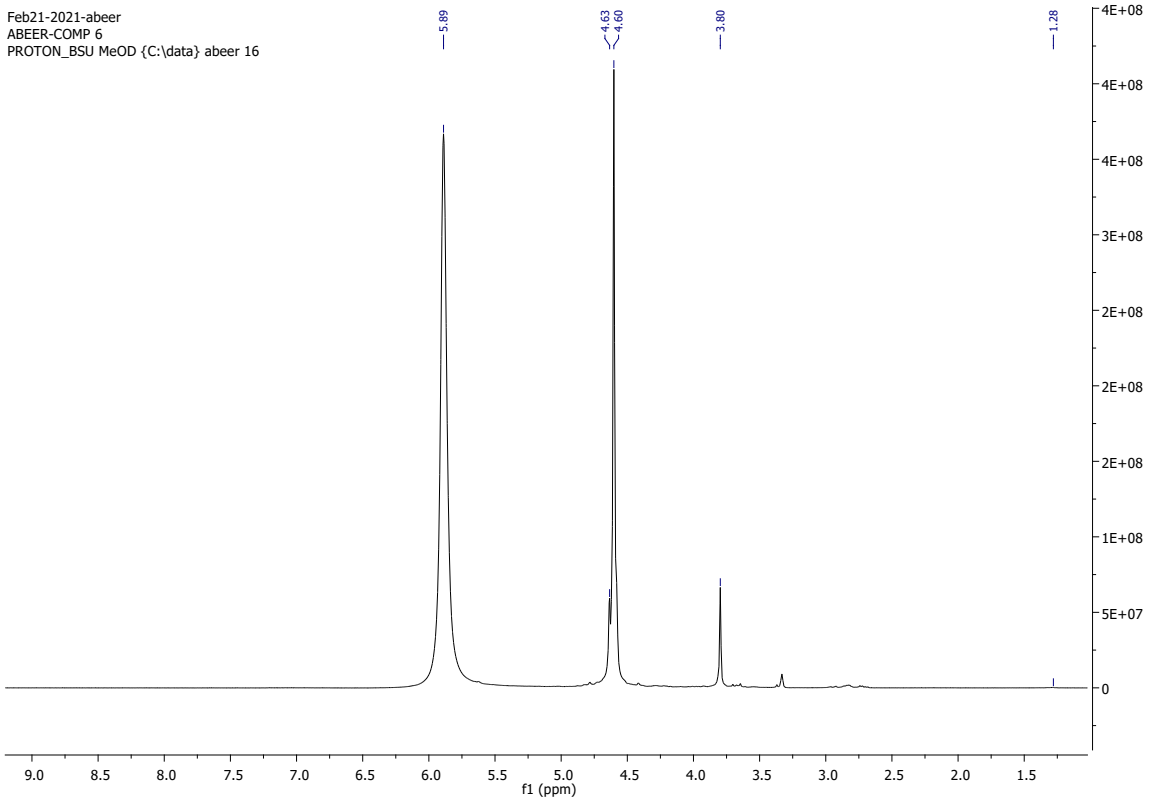

Figure S9. ^{1}H NMR spectrum of compound **5** measured in CD_3OD-d_4 at 400 MHz

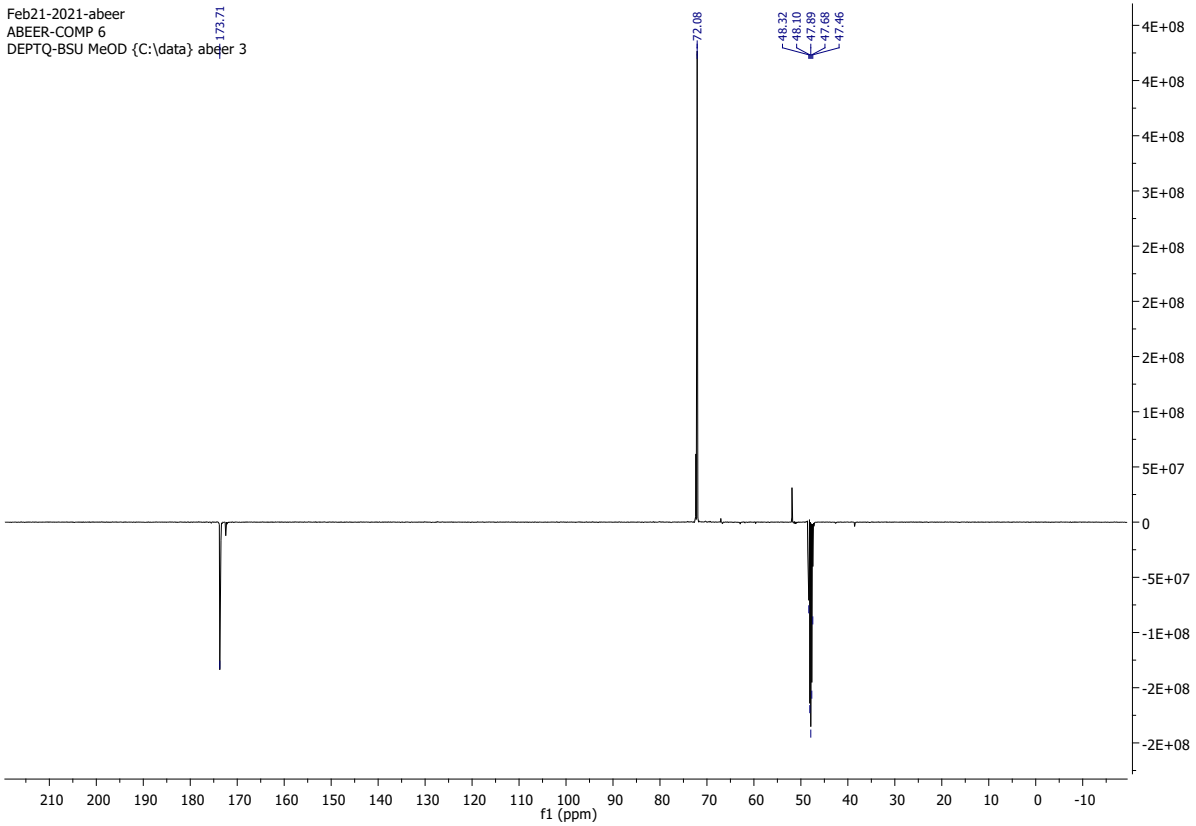

Figure S10. DEPT-Q NMR spectrum of compound **5** measured in CD_3OD-d_4 at 100 MHz

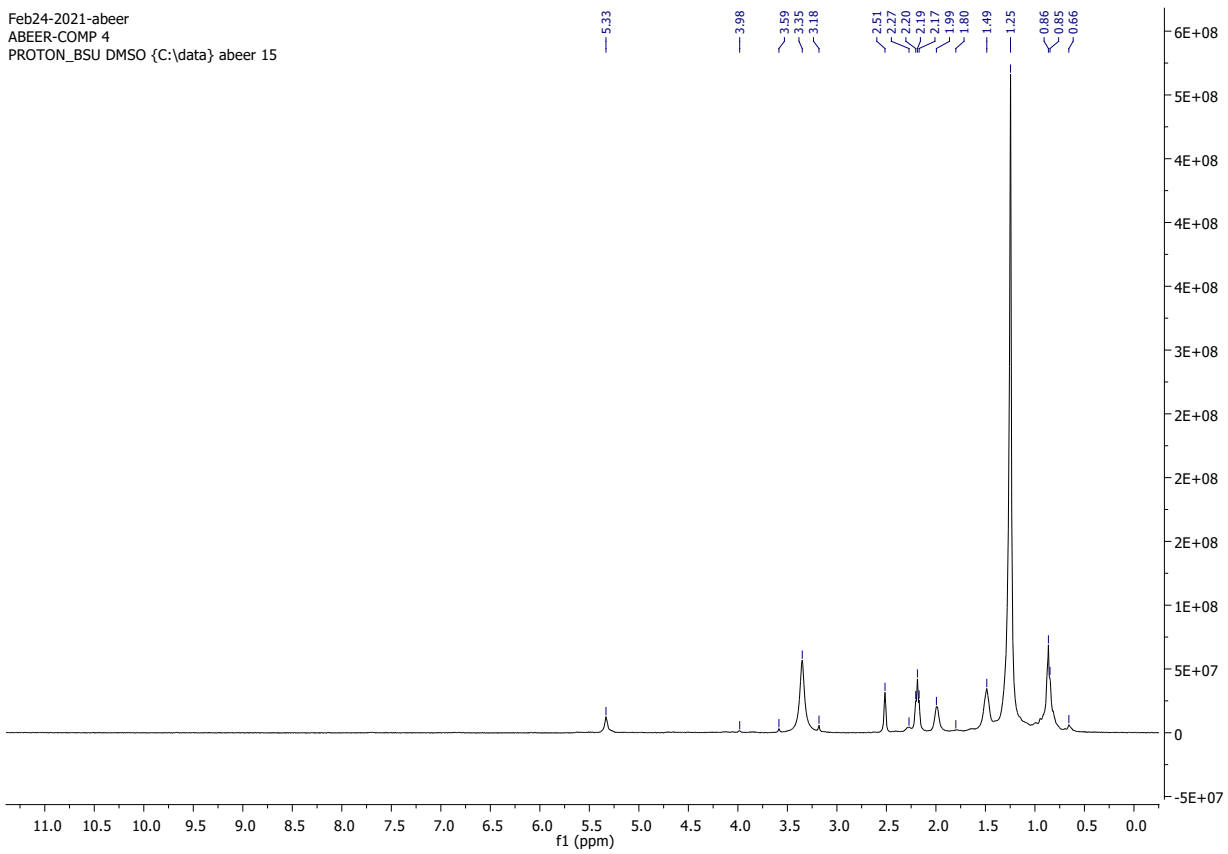

Figure S11. ^{1}H NMR spectrum of compound **6** measured in DMSO-d_6 at 400 MHz

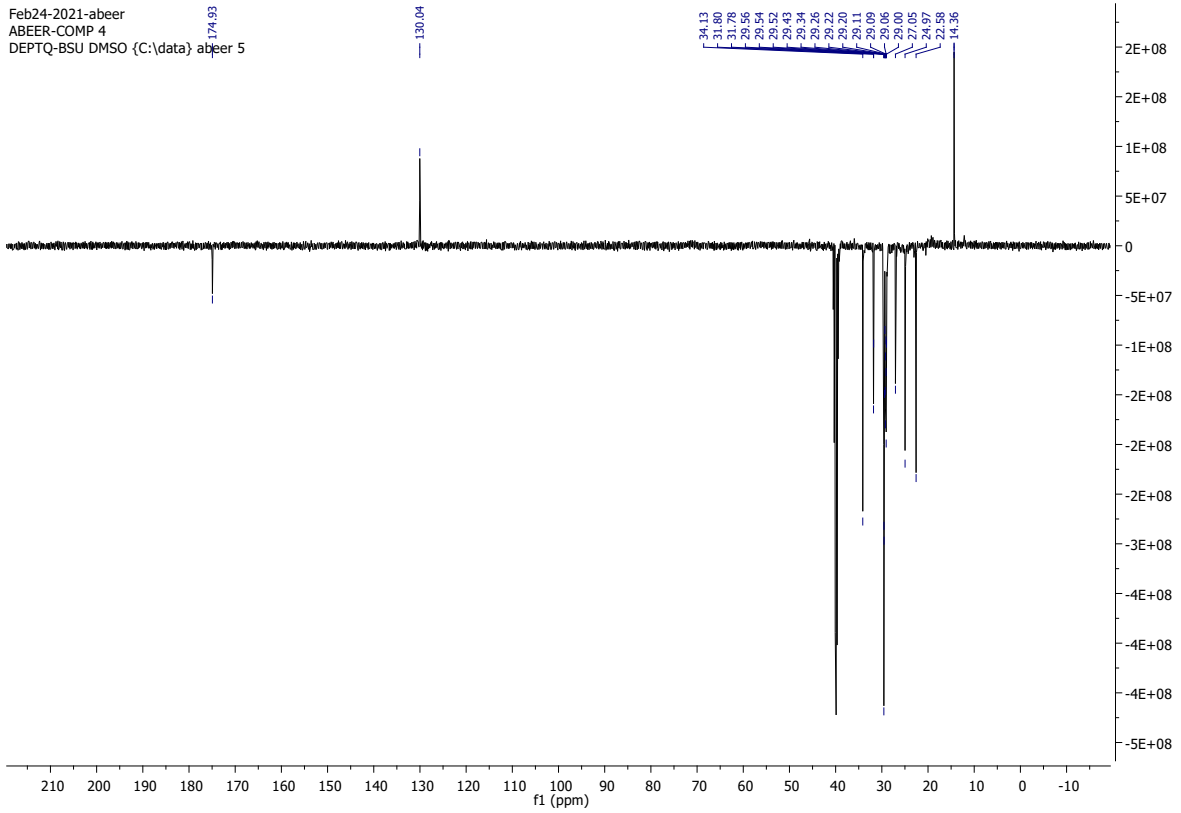

Figure S12. DEPT-Q NMR spectrum of compound **6** measured in DMSO-d_6 at 100 MHz

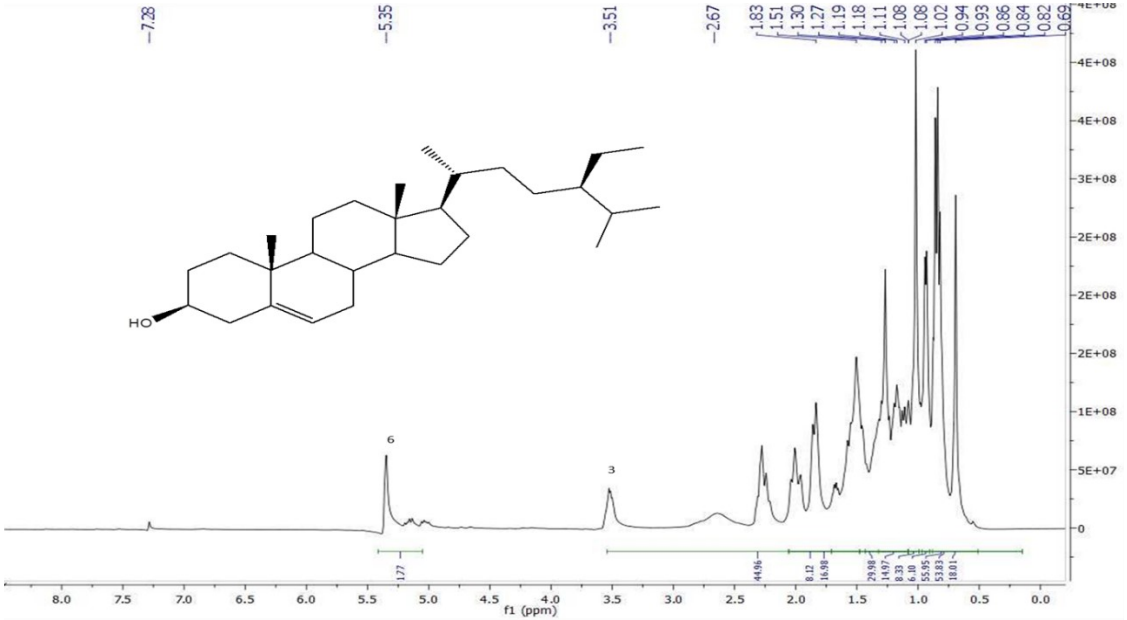

Figure S13. ^{1}H NMR spectrum of compound **7** measured in $CDCL_3$-*d* at 400 MHz

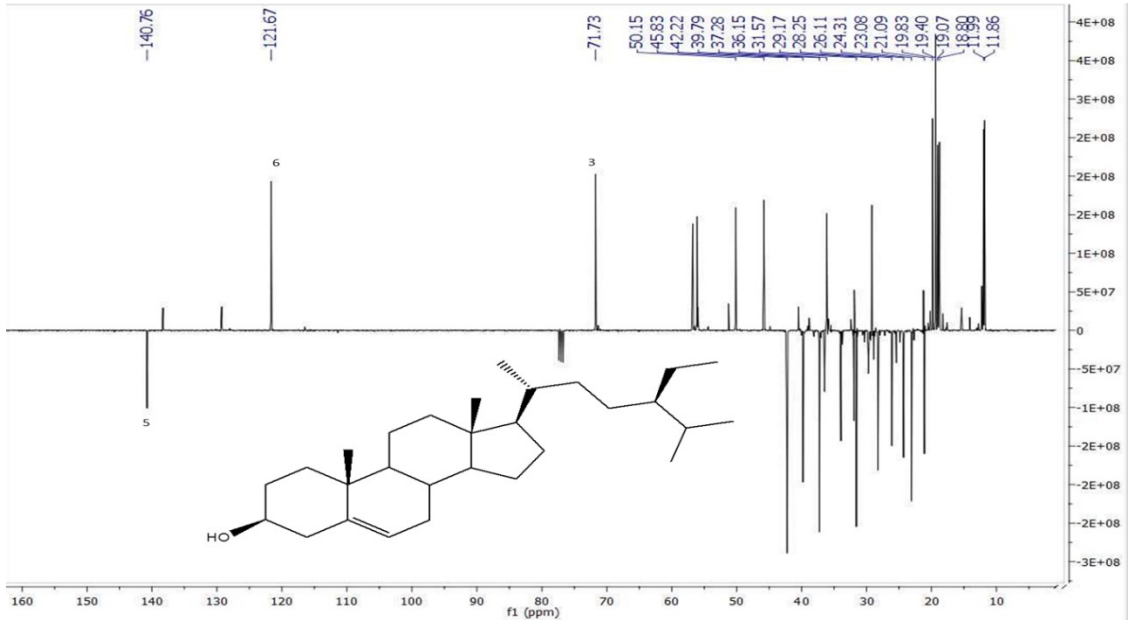

Figure S14. DEPT-Q NMR spectrum of compound **7** measured in $CDCL_3$-*d* at 100 MHz

Methods

***Prediction of the Potential Protein Targets of the annotated Compounds in T. indica* crude extract**

By performing inverse docking against all human proteins in the Protein Data Bank (PDB; https://www.rcsb.org/), potential protein targets for the annotated compounds in *T. indica* crude extract were identified. This task was accomplished with the help of the idTarget platform (http://idtarget.rcas.sinica.edu.tw/). This structural-based screening software uses a unique docking approach known as divide-and-conquer docking, in which it adaptively builds small overlapping grids to constrain the searching space on protein surfaces, allowing it to run a large number of accurate docking experiments in a shorter amount of time. The data were collected as a list of binding affinity scores, organized from the most negative to the least negative. To identify the optimal targets for each identified molecule in *T. indica* crude extract, we used a binding affinity score of -7 kcal/mol as a cut-off number. Accordingly, AchE (PDB: 4EY6) was selected as an Alzheimer-related target for compounds 1 and 2.

Molecular Docking

AutoDock Vina software was used in all molecular docking experiments[1]. All annotated compounds were docked against the AchE crystal structure (PDB codes: 4EY6)[2] . The binding site was determined according to the enzyme's co-crystallized ligand. The co-ordinates of the grid box were: x = -10.77; y = -42.48; z = 30.56. The size of the grid box was set to be 10 Å. Exhaustiveness was set to be 24. Ten poses were generated for each docking experiment. The top-scoring poses were selected for MDS. Docking poses were analyzed and visualized using Pymol software[1].

Molecular Dynamics Simulation

Desmond v. 2.2 software was used for performing MDS experiments[3-5]. This software applies the OPLS-2005 force field. Protein systems were built using the System Builder option, where the protein structure was checked for any missing hydrogens, the protonation states of the amino acid residues were set (pH = 7.4), and the co-crystalized water molecules were removed. Thereafter, the whole structure was embedded in an orthorhombic box of TIP3P water together with 0.15 M Na+ and Cl− ions in 20 Å solvent buffer. Afterward, the prepared systems were energy minimized and equilibrated for 10 ns. For proteinligand complexes, the top-scoring poses were used as a starting points for simulation. Desmond software automatically parameterizes inputted ligands during the system building step according to the OPLS force field. For simulations performed by NAMD[6], the protein structures were built and optimized by using the QwikMD toolkit of the VMD software. The parameters and topologies of the compounds 1 and 2 were calculated using the VMD plugin Force Field Toolkit (ffTK). Afterward, the generated parameters and topology files were loaded to VMD to readily read the protein–ligand complexes without errors and then conduct the simulation step.

Binding Free Energy Calculations

Binding free energy calculations (ΔG) were performed using the free energy perturbation (FEP) method[7]. This method was described in detail in the recent article by Kim and coworkers[7]. Briefly, this method calculates the binding free energy $\Delta G_{binding}$ according to the following equation: $\Delta G_{binding} = \Delta G_{Complex} - \Delta G_{Ligand}$. The value of each ΔG is estimated from a separate simulation using NAMD software. All input files required for simulation by NAMD can be prepared by using the online website Charmm-GUI (https://charmm-gui.org/?doc=input/afes.abinding, accessed on 23 June 2021). Subsequently, we can use these files in NAMD to produce the required simulations using the FEP calculation function in NAMD. The equilibration (5 ns long) was achieved in the

NPT ensemble at 300 K and 1 atm (1.01325 bar) with Langevin piston pressure (for "Complex" and "Ligand") in the presence of the TIP3P water model. Then, 10 ns FEP simulations were performed for each compound, and the last 5 ns of the free energy values were measured for the final free energy values[7]. Finally, the generated trajectories were visualized and analyzed using VMD software.

References

1. D. Seeliger and B. L. de Groot, *Journal of computer-aided molecular design*, 2010, **24**, 417-422.
2. F. J. Moy, P. K. Chanda, J. M. Chen, S. Cosmi, W. Edris, J. S. Skotnicki, J. Wilhelm and R. Powers, *Biochemistry*, 1999, **38**, 7085-7096.
3. K. J. Bowers, D. E. Chow, H. Xu, R. O. Dror, M. P. Eastwood, B. A. Gregersen, J. L. Klepeis, I. Kolossvary, M. A. Moraes and F. D. Sacerdoti, 2006.
4. S. Release, *Maestro-Desmond Interoperability Tools, Schrödinger, New York, NY*, 2017.
5. V. Maestro, *Schrödinger, LLC: New York, NY, USA*, 2009.
6. J. C. Phillips, R. Braun, W. Wang, J. Gumbart, E. Tajkhorshid, E. Villa, C. Chipot, R. D. Skeel, L. Kale and K. Schulten, *Journal of computational chemistry*, 2005, **26**, 1781-1802.
7. S. Kim, H. Oshima, H. Zhang, N. R. Kern, S. Re, J. Lee, B. Roux, Y. Sugita, W. Jiang and W. Im, *Journal of chemical theory and computation*, 2020, **16**, 7207-7218.